

1 **Saline groundwater evolution in Luanhe River Delta, China since**

2 **Holocene: hydrochemical, isotopic and sedimentary evidence**

3 Xianzhang Dang^{a, b, c}, Maosheng Gao^{b, d}, Zhang Wen^a, Guohua Hou^{b, d}, Hamza Jakada^e,

4 Daniel Ayejoto^a, Qiming Sun^{a, b, c}

5 ^aSchool of Environmental Studies, China University of Geosciences, 388 Lumo Rd,

6 Wuhan, 430074, China

7 ^bQingdao Institute of Marine Geology, CGS, Qingdao, 266237, China

8 ^cChinese Academy of Geological Sciences, Beijing, 100037, China

9 ^dLaboratory for Marine Geology, Pilot National Laboratory for Marine Science and

10 Technology, Qingdao, 266237, China

11 ^eDepartment of Civil Engineering, Baze University Abuja, Nigeria

12 *Correspondence to:* Maosheng Gao (gaomsh66@sohu.com), Zhang Wen

13 (wenz@cug.edu.cn)

14

1 **Abstract**

2 Since the Quaternary Period, palaeo-seawater intrusions have been suggested to explain
3 the observed saline groundwater that extends far inland in coastal zones. The Luanhe
4 River Delta (northwest coast of Bohai Sea, China) is characterized by the distribution
5 of saline, brine, brackish and fresh groundwater, from coastline to inland, with a wide
6 range of total dissolved solids (TDS) between 0.38-125.9 g/L. Meanwhile, previous
7 studies have revealed that this area was significantly affected by Holocene marine
8 transgression. This study used hydrochemical, isotopic, and sedimentological methods
9 to investigate groundwater salinization processes in the Luanhe River Delta and its links
10 to the palaeo-environmental settings. The isotopic results (^2H , ^{18}O , ^{14}C) facilitate the
11 distinction between old and new groundwater recharge. The hydro-chemical analysis
12 using PHREEQC indicates that the origin of salt in saline and brine groundwater is
13 from a marine source. The ^{18}O -Cl relationship diagram yields three end-member
14 groundwater mixing with two mixing scenarios suggested to explain the freshening and
15 salinization processes in the study area. When interpreted with data from palaeo-
16 environmental sediments, we found that groundwater salinization may have occurred
17 since the Holocene marine transgression. The brine is characterized by radiocarbon
18 activities of ~50 to 85 pMC and relatively depleted stable isotopes, which is associated
19 with seawater evaporation in the ancient lagoon during delta progradation and mixing
20 with deeper fresh groundwater which probably was recharged in cold late Pleistocene.
21 As for the brackish and fresh groundwater are characterized by river-like stable isotope
22 values where high radiocarbon activities (74.3 to 105.9 pMC) were formed after the

1 wash-out of salinized aquifer by surface water in the delta plain. This study presents an
2 approach for utilizing geochemical indicator analysis with paleogeographic
3 reconstruction to better assess groundwater evolutionary patterns in coastal aquifers.
4

1 **Introduction**

2 It is estimated that around 40% of the world's population lives in coastal areas (UN
3 Atlas, 2010). Groundwater is an important freshwater resource for domestic
4 consumption and agricultural activities in this region (Cary et al., 2015; Jayathunga et
5 al., 2020). However, groundwater salinization poses a significant threat to everyday
6 living and development activities (Tulipano, 2005; de Montety et al., 2008). In recent
7 decades, groundwater salinization in coastal zones are widely concerned and studied.
8 On the one hand, seawater intrusion due to groundwater pumping is a vital salinization
9 process in the coastal aquifer (Reilly and Goodman, 1985; Werner, 2010, 2013; Han
10 and Currell, 2018). On the other hand, groundwater salinization caused by the palaeo-
11 seawater intrusion, in response to the Quaternary changes in global sea-level, has been
12 reported in many coastal zones worldwide (Edmunds, 2001; Akouvi, 2008; Santucci et
13 al., 2016, Larsen et al., 2017).

14 Coastal aquifers are linked to the ocean and continental hydrological cycle (Ferguson
15 and Gleeson, 2012), both of which are influenced by natural and human-induced change
16 (Jiao and Post, 2019). There is a steady-state seawater-freshwater interface under the
17 natural state that extends inland from the coastal line (Costall et al., 2020). Since the
18 Quaternary period, however, sea-level fluctuations on geological timescales have
19 caused the interface to change, allowing seawater intrusion during transgression events
20 and freshwater flushing during glacial low sea-level periods, which are evident in
21 hydrochemical characteristics of groundwater in coastal aquifers(Kooi et al., 2000;
22 Sanford, 2010; Aquilina et al., 2015; Lee et al., 2016). In addition, the hypersaline

1 groundwater found in coastal zones, particularly brine groundwater with a salinity of
2 2-4 times that of seawater, cannot be explained solely by using a seawater intrusion
3 model (Sola et al., 2014, Han et al., 2020), and palaeoenvironment settings must be
4 taken into consideration (Van Engelen et al., 2019). Some studies, for example, attribute
5 the presence of brine in Mediterranean countries to the evaporation of seawater in the
6 lagoon system during the Holocene transgression (Giambastiani et al., 2013, Vallejos
7 et al., 2018).

8 The Bohai Sea of northern China was affected by Late Pleistocene transgressive-
9 regressive cycles, which caused various salinity palaeo-saltwater intrusion along the
10 coastal aquifers (Du et al., 2015; Li et al., 2017). Several studies have applied
11 geochemical methods to elucidate the origin of saline groundwater and the salinization
12 processes under anthropogenic influence, including induced mixing brine water from
13 adjacent aquifers caused by groundwater overexploitation in Laizhou Bay (Han et al.,
14 2011, 2014; Liu et al., 2017; Qi et al., 2019). However, the association between
15 groundwater salinization (especially brine formation) and palaeoenvironmental
16 implications are still not clear. Thus, this study applies a range of chemical, isotopic
17 and sedimentary indicators to examine the Luanhe River Delta (situated along the
18 northwestern coast of Bohai Sea) to elucidate the groundwater salinization processes in
19 relation to recharge, salt source, mixing behavior and palaeogeographic evolution. The
20 overall goal is to understand the groundwater evolutionary pattern influenced by
21 transgression/regression events in geologic time. The findings will be significant to
22 aquifer remediation activities in the region as well as other similar sedimentary

1 environments around the world.

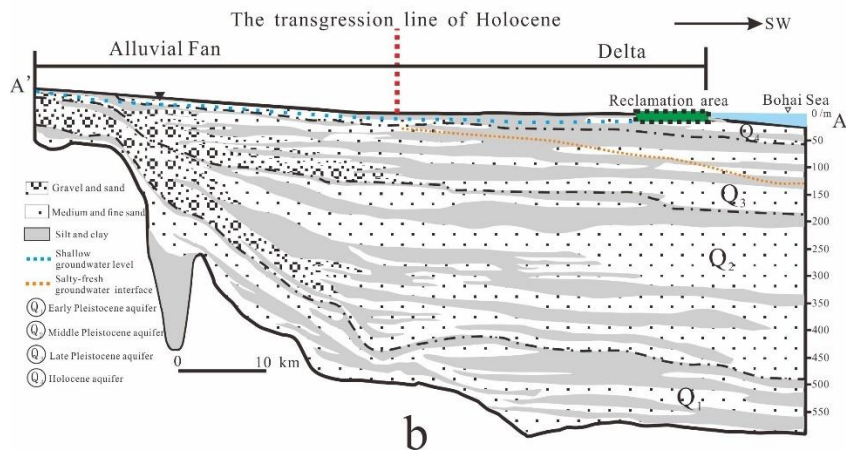
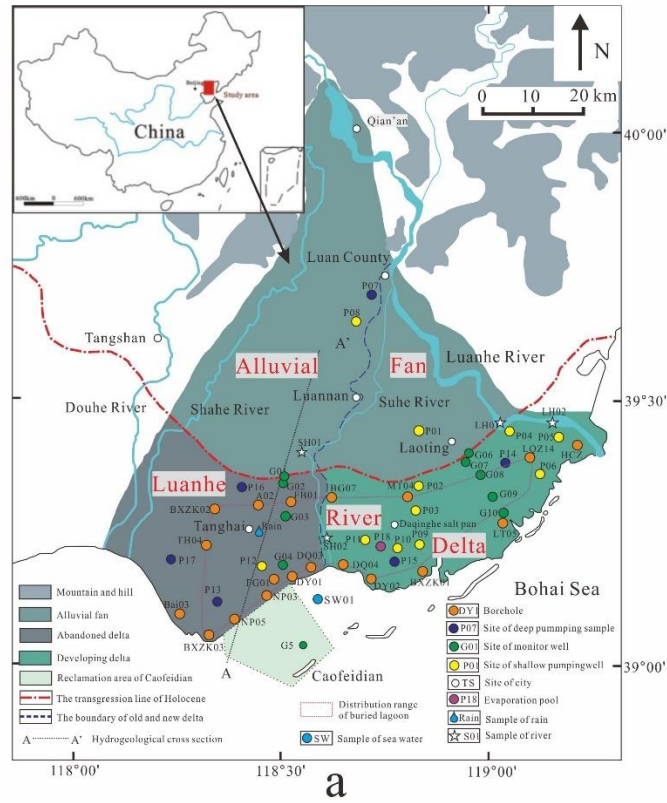
2 **2 Background of the study area**

3 The study area is located in northeastern Hebei Province, China, on the west coast of
4 Bohai (Fig. 1a). The study area consists of alluvial fan and coastal delta, bounded by
5 Holocene maximum transgression line (Xue, 2016). The delta area can be further
6 divided into two parts: old delta between the Douhe River and the Suhe River, the new
7 delta between the Suhe River and the modern Luanhe River (He et al., 2020). The
8 geomorphology of the study area is inclined to the south and southwest with a slope of
9 about 0.04-2‰. The temperate monsoon climate affects the average annual temperature
10 of 12.5°C and annual rainfall of 601 mm (1956-2010), with 80% of the annual rainfall
11 occurring between July and September.

12 2.1 Hydrogeology

13 The thickness of Quaternary sediments in the study area is about 400-500 m.
14 According to the lithology and hydrogeological characteristics, the Quaternary aquifers
15 are made up of four distinct aquifers (Fig. 1b): The First Holocene aquifer (Q_4) is a
16 phreatic or semi-confined aquifer with a bottom depth of 15-30 m and is primarily
17 composed of fine sand and slit, involving fresh, brackish, saline and brine groundwater
18 (Dang et al., 2020). The second Late Pleistocene aquifer (Q_3), the third Middle
19 Pleistocene aquifer (Q_2), and the fourth Early Pleistocene aquifer (Q_1), with bottom
20 depths of 120-170 m, 250-350 m, and 350-550 m, respectively. They have confined
21 aquifers primarily made up of medium sand and gravel (Niu et al., 2019). The first
22 aquifer is mainly recharged by meteoric precipitation and lateral infiltration of surface

1 water (Li et al., 2013). The groundwater from the first aquifer is widely extracted for
2 irrigation in the alluvial fan areas. The largest salt farm in north China, the Daqinghe
3 Salt Farm, uses shallow brine groundwater for salt production in the delta area, where
4 agricultural activities are small. Except for the area of alluvial fan, the circulation
5 between phreatic and confined aquifers is weak. The deep groundwater in second, third,
6 and fourth aquifers are mainly recharged by a surrounding mountain range and mainly
7 discharged by human pumping (Ma et al., 2014).



1

2 Fig. 1. (a) Location map of study area. Also shown are the sampling site and published cores in the

3 Luanhe River Delta. Cores LT05, HCZ, BXZK01, BXZK02 and BXZK03 were cited from He et

4 al. (2020); Cores NP05, NP03, DY01, DQ03, DQ04, DY02, MT04, BG07, FB01, A02 and TH04

5 were cited from Xu et al. (2020); Core LQZ04 was cited from Cheng et al. (2020); Core FG01 was

6 cited from Xu et al. (2011); Core Bai03 was cited from Li and Wang. (1983); Core HCZ was cited

7 from Peng et al. (1981). (b) Hydrogeological cross-section (A-A' in Fig. 1a) of study area,

8

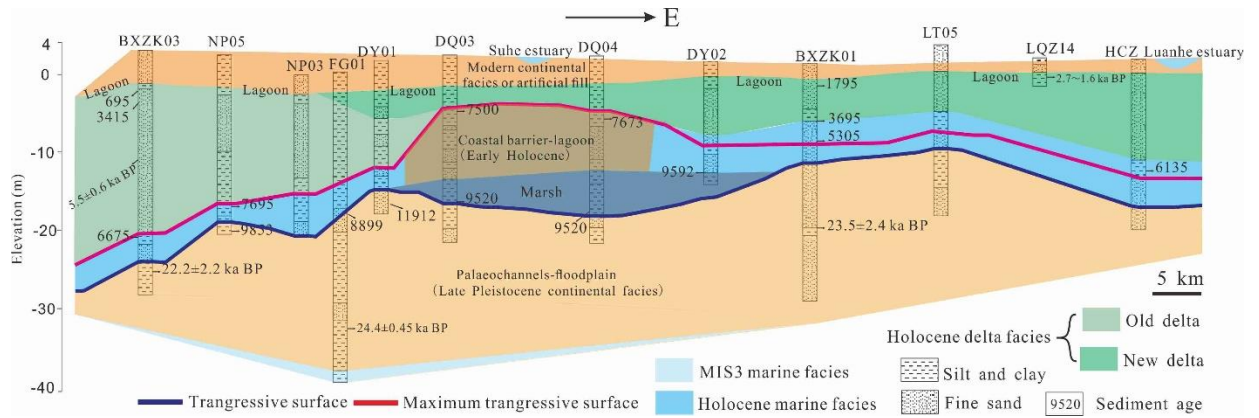
modified by Ma et al., 2014.

1 2.2 Sedimentary evolution since the Late Pleistocene

2 Previous studies have shown that in the study region, the interface of salt-fresh
3 groundwater gradually deepens from land (depth of ~ -5 m) to sea (depth of ~ -100 m),
4 as shown in Fig. 1b, with salt groundwater primarily occurring in the first aquifer of the
5 delta area (Li et al., 2013; Ma et al., 2014). According to stratigraphic transect along
6 the present coastline (Fig. 2), the series stratigraphic architecture of the first aquifer
7 consists of Late Pleistocene continental facies - Holocene marine facies – Holocene
8 delta facies - modern continental facies or artificial fill, indicating that the sediments of
9 the first aquifer had been deposited from lowstand continental accumulation to marine
10 transgression and high stand progradation since the Late Pleistocene.

11 The seawater had not reached the modern coastline from the Last Glacial Maximum
12 to the early Holocene (about 30-9 ka B.P.). The Luanhe alluvial fan was an activity in
13 this period (He et al., 2020). Since about 9000 a B.P., the Holocene marine transgression
14 approached the present coastline (Xu et al., 2020), and Holocene marine sediments
15 developed under the sea-level rise from 9-7 ka B.P. The Holocene marine transgression
16 had reached its maximum inland area 20 km from the modern coastline until about 7 ka
17 B.P. (Gao et al., 1981; Peng et al., 1981; Xue, 2014, 2016) (Fig. 1 transgression line of
18 Holocene), the accumulation of highstand prograding delta on top of Holocene marine
19 strata, together with the artificial fill formed the modern coastal plain. In addition,
20 lagoons are important components of the Luanhe River Delta (Feng and zhang, 1998).
21 According to the records of lagoon facies in the published cores in this region, the
22 approximate distribution range of buried lagoon is shown as a purple dashed line in Fig.

1 1a.



2

3 Fig.2 Stratigraphic transect along the present coastline of Luanhe River Delta, modified from He

4

et al.,2020.

5 3 Methods

6 In total, 45 water samples were collected from the Luanhe River Delta, including
7 38 groundwater samples, 5 surface water samples, 1 local rain water and 1 Bohai
8 seawater samples, during 4 sampling campaigns from October 2016 to June 2020.
9 Groundwater samples were divided into shallow groundwater samples and deep
10 groundwater samples, which were pumped from unconfined aquifer and confined
11 aquifer respectively. Surface water includes 2 Suhe River water samples and 2 Luanhe
12 River water samples. Due to artificial fill that has modified the coastal landscape, it was
13 difficult to locate the modern lagoon environment. However, during the investigation,
14 it was found that the Daqinghe salt farm in this area extracts seawater into the
15 evaporation pond. The mixture of seawater and meteoric water is subject to evaporation
16 to form concentrated saline water (CSW) in the pond, which is similar to the formation
17 of CSW in a coastal lagoon (Stumpp et al., 2014). Thus, 1CSW (P18 sample) in the
18 evaporation pond was collected.

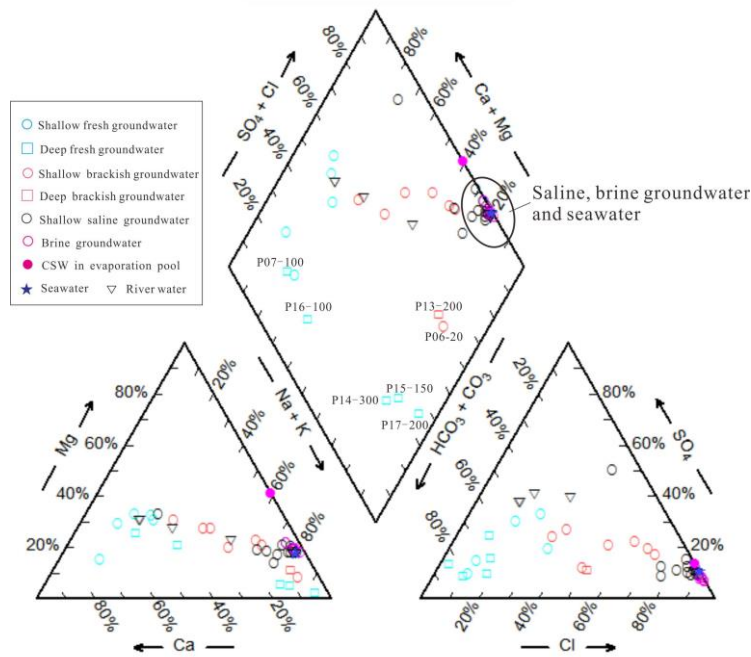
1 Water types were classified according to Zhou (2013): freshwater (TDS < 1 g/L),
2 brackish water (TDS = 1 to 3 g/L), saline water (TDS = 3 to 50 g/L), and brine (TDS >
3 50 g/L). Groundwater sampling depths and pH values were measured on site using
4 CDT-divers. The concentrations of K⁺, Na⁺, Ca²⁺, Mg²⁺, and Br⁻ ion were measured
5 using inductively coupled plasma analysis (ICAP-7400), while SO₄²⁻ and Cl⁻ ions were
6 determined using ion chromatography (ICS-600). The HCO₃⁻ concentrations of samples
7 were measured using titration. The hydrochemical data are listed in Table S1(see
8 Supplement). The stable isotope concentrations (δ D, δ ¹⁸O) of the water samples
9 (including G02-10, G06-10, G03-05, G04-40, G05-10, G05-46, G07-27, P07-20, P08-
10 30, P09-30, P10-30, P11-20, P12-40 P14-15, P07-100, P13-200, P14-300, P15-150,
11 P16-100, P17-200, P18, LH01, LH02, SH01, SH02, SW01, R1) were tested at the
12 Experimental & Testing Center of Marine Geology, Ministry of Natural Resource,
13 China, using High Temperature Pyrolysis-Isotope Ratio Mass Spectrometry. The values
14 of δ ¹⁸O and δ D were calculated with respect to the Vienna Standard Mean Ocean Water
15 (VSMOW), and the uncertainty for δ D and δ ¹⁸O are $\pm 1.0\%$ and $\pm 0.2\%$, respectively.
16 The radioisotope (AMS ¹⁴C) of groundwater samples (P14-300, P15-150, and P16-100)
17 were measured at the Pilot National Laboratory for Marine Science and Technology.
18 Stable isotopes (δ D, δ ¹⁸O, ¹³C) and radioisotope of groundwater samples (G10-10,
19 G03-20, G04-15, G05-30, G06-15, G07-15, G08-15, G08-40, G09-15, G09-40, G10-
20 10, G10-30) were analyzed at the Beta Analytic TESTING LABORATORY, where the
21 δ ¹⁸O and δ D values were also calculated with respect to VSMOW, and the uncertainty
22 for δ D and δ ¹⁸O are listed in Table S1. The ¹⁴C age of groundwater was calculated

1 using the following equation: $t = -8267 \cdot \ln(a_t^{14C}/q \cdot a_0^{14C})$ (Clark and Fritz, 1997),
2 where t is radiocarbon ages in years Before Present (a B.P.); a_t^{14C} is the measured 14C
3 activity in % of modern carbon (pMC); a_0^{14C} is the modern 14C activity of soil derived;
4 q is a corrective factor, the corrective factor accounts for the dissolution of calcite,
5 which is assumed to be free of 14C and, therefore, dilutes the initial 14C activity of
6 aqueous DIC in recharged water. The results of 13C , 14C and the uncorrected residence
7 times are listed in Table S2.

8 **4 Results**

9 4.1 Hydrochemistry

10 Except for P13-200 (TDS=1.617 g/L, which is brackish water), all the deep
11 groundwater samples in the study region are freshwater. Deep groundwater
12 hydrochemical forms shift from Ca-HCO₃ to Na-HCO₃ as it moves from land to sea
13 (Fig. 3). For shallow aquifer, the horizontal interface of salt-fresh groundwater
14 corresponds better with the maximum Holocene transgression line (see Fig. 1a). The
15 Ca-HCO₃ type of shallow fresh groundwater is primarily distributed in the alluvial fan
16 region. The brackish and low TDS saline groundwater, which vary from Ca-HCO₃, Na-
17 HCO₃, and Na-Cl types, are mainly contained in the upper aquifer (depth of 0-15 m) of
18 delta area, while the lower part (depth of 20–40 m) is Na-Cl type of saline and brine
19 groundwater with high TDS. Moreover, for horizontal distribution of salinity, the
20 groundwater TDS tends to decrease from west to east, such as the TDS of saline and
21 brine groundwater TDS generally range from 16.57–125.97 g L⁻¹ in old delta (western
22 delta), while 3.26–52.48 g L⁻¹ in the new delta (eastern delta).



1

2

Fig. 3 Piper diagram of the various water samples.

3

4.2 ^2H , ^{18}O stable isotopes

4

5

6

7

8

9

10

11

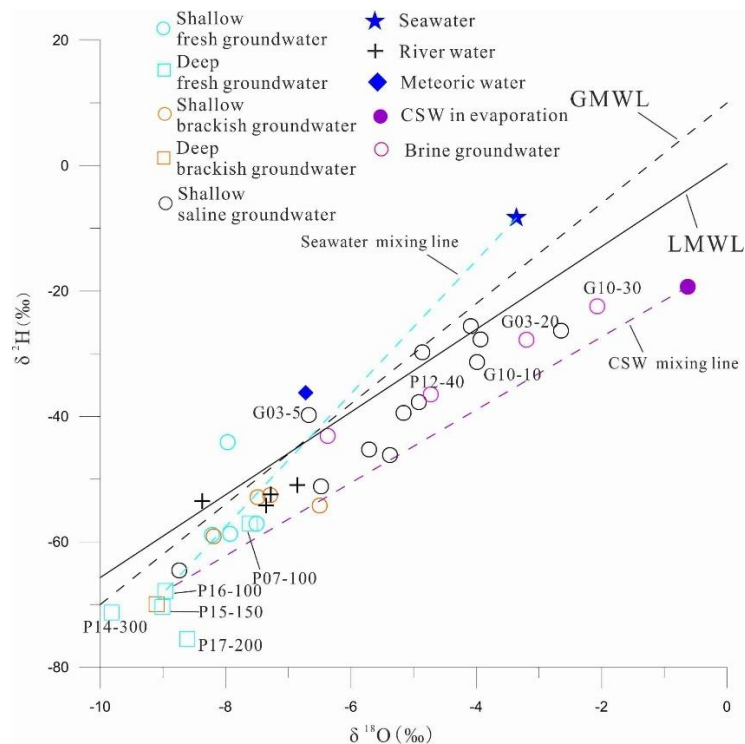
12

13

14

Fig. 4 shows the relationship between deuterium and oxygen-18. The global meteoric water line (GMWL, $\delta^2\text{H}=8\cdot\delta^{18}\text{O}+10$) is cited from Craig (1961), while the local meteoric water line (LMWL, $\delta^2\text{H}=6.6\cdot\delta^{18}\text{O}+0.3$) is based on $\delta^2\text{H}$ and $\delta^{18}\text{O}$ isotope data (1985-2003, mean monthly rainfall values) from the Tianjin station, about 100 km southwest of the study area (IAEA/WMO, 2006). The deep groundwater samples exhibit depleted values of stable isotopes, with values of $\delta^2\text{H}$ ranging from -75.52‰ to -57.06‰ and $\delta^{18}\text{O}$ from -9.82‰ to -7.61‰. Shallow groundwater samples have heavier hydrogen and oxygen isotope levels, ranging from -64.6 to -22.46‰ for $\delta^2\text{H}$ and -8.74 to -2.07‰ for $\delta^{18}\text{O}$. While the relatively small overall value of fresh and brackish groundwater samples are similar to those of the river samples, saline and brine groundwater, were generally plotted below the LMWL or GMWL, which mean that the

1 water was subjected to evaporation prior to recharge into groundwater (Gibson et al.,
 2 1993), or that multiple end-members mixing processes were involved (Han et al., 2011).



3
 4 Fig. 4 Stable isotope compositions of different water samples. Seawater mixing line: mixing
 5 between deep fresh groundwater and seawater; CSW mixing line: mixing between deep fresh
 6 groundwater and CSW.

7 4.3 Groundwater residence times

8 The measured ^{14}C activities of groundwater samples range from 0.774 to 105.9 pMC
 9 (Table S2). The properties of ^{14}C and sampling depth is shown in Fig. 5, which
 10 elucidates the negative correlations, showing that variations of ^{14}C activities could be
 11 attributed to radioactive decay aquifer. There are multiple processes that can impact the
 12 ^{14}C properties including groundwater mixing and dispersion, long-term variation of
 13 atmospheric ^{14}C and free ^{14}C dilution (e.g. carbonate dissolution) (Cartwright et al.,
 14 2020). Due to the relative impact of these processes (which are not well established in

1 the study area), the uncertainty regarding the correction of radiocarbon ages to real
2 groundwater ages is very high. Consequently, we estimate groundwater age as a range
3 of the residence time. Uncorrected ages are considered the maximum age, while
4 corrected ages are the minimum age that are determined based on two hypothetical
5 models on carbonate dissolution that mainly affect the ^{14}C contents of water samples
6 (Lee et al., 2016).

7 Fig.5 shows activities of the ^{14}C in the shallow groundwater are within 30.6 to 105.9
8 pMC. These values indicate relatively modern recharge before atmospheric nuclear
9 testing period of the 1950s and 1960s. The radiocarbon activities in the deep fresh
10 groundwater are less than 12 pMC, which is consistent with the palaeo-water recharge.
11 This indicates that there are weak connection between shallow and deep aquifers.
12 Therefore, we assume that the shallow aquifer is an open system, while the deep aquifer
13 is a closed system. The $\delta^{13}\text{C}$ mixing and chemical mass balance (CMB) models are used
14 to estimate to corrective factor q , respectively (Clark and Fritz, 1997).

15 For $\delta^{13}\text{C}$ mixing model, $q = (\delta^{13}\text{C}_{\text{DIC}} - \delta^{13}\text{C}_{\text{CARB}}) / (\delta^{13}\text{C}_{\text{RECH}} - \delta^{13}\text{C}_{\text{CARB}})$
16 (Pearson and Hanshaw, 1970), where $\delta^{13}\text{C}_{\text{DIC}}$ is the measured $\delta^{13}\text{C}$ of DIC in
17 groundwater; $\delta^{13}\text{C}_{\text{CARB}}$ is the $\delta^{13}\text{C}$ of DIC from dissolved soil mineral, using $\delta^{13}\text{C}_{\text{CARB}}$
18 = 1.5 ‰ (Chen et al., 2003); $\delta^{13}\text{C}_{\text{RECH}}$ is the $\delta^{13}\text{C}$ in water when it reaches the saturation
19 zone. In this study, we use a $\delta^{13}\text{C}_{\text{RECH}}$ of -15 ‰, which has been suggested as
20 appropriate for soils in northern China dominated by C_4 plants (Currell et al., 2010).
21 The model yielded some relatively low q values (0.59 of G06-15 and 0.65 of G08-15),
22 possibly since several unaccounted factors would contribute to variable $\delta^{13}\text{C}_{\text{RECH}}$ values,

1 e.g. local methanogenesis and pH or temperatures in the soil zones.

2 For CMB, $q = \text{mDIC}_{\text{rech}} / \text{mDIC}_{\text{final}}$, where $\text{mDIC}_{\text{rech}}$ is the DIC molar concentration
3 in the recharging water and $\text{mDIC}_{\text{final}}$ is the DIC molar concentration in the final
4 groundwater. $\text{mDIC}_{\text{final}}$ was calculated using:

5 $\text{mDIC}_{\text{final}} = \text{mDIC}_{\text{rech}} + [\text{mCa} + \text{Mg} - \text{SO}_4 + 0.5(\text{Na} + \text{K} - \text{Cl})]$ (Fontes and Garnier,
6 1979). DIC_{rech} was mainly HCO_3 in the recharged water when pH values were between
7 6.4 and 10.3, and the carbonate equilibrium constant varies with temperature (Clark and
8 Fritz, 1997). $\text{mDIC}_{\text{rech}}$ was calculated from estimated pH and temperature condition for
9 the recharge environment, e.g., at pH = 6 and T = 15°C, the $\text{mDIC}_{\text{rech}} = 10$ mmol/L
10 (Currell et al., 2010).

11 The corrected radiocarbon ages are shown in Table S2. The residence time of deep
12 groundwater ranged from 15959-39050 a B.P., which is significantly longer than that
13 of groundwater in the shallow aquifer (9510 a B.P. to modern). Moreover, most brackish
14 and fresh groundwater ages are modern, while brine has a longer residence period
15 (5590-1245 a B.P.) and a broader variety of saline groundwater samples.

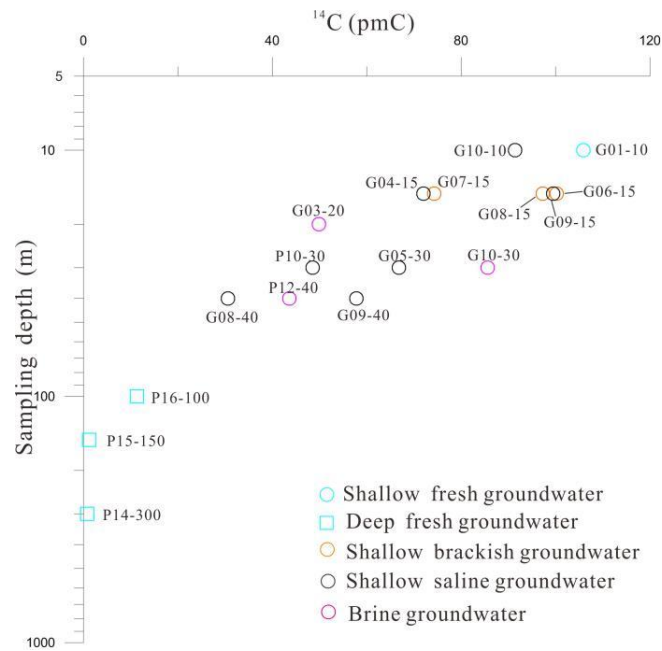


Fig. 5 ¹⁴C activity with sampling depth in groundwater.

5 Discussion

5.1 Isotopic analysis for origin and recharge of groundwater

Deuterium and oxygen-18 are good tracers for groundwater origin and climatic conditions during recharge periods (Clark and Fritz, 1997). When combined with groundwater residence time, they could further identify modern and palaeo recharge (Han et al., 2014).

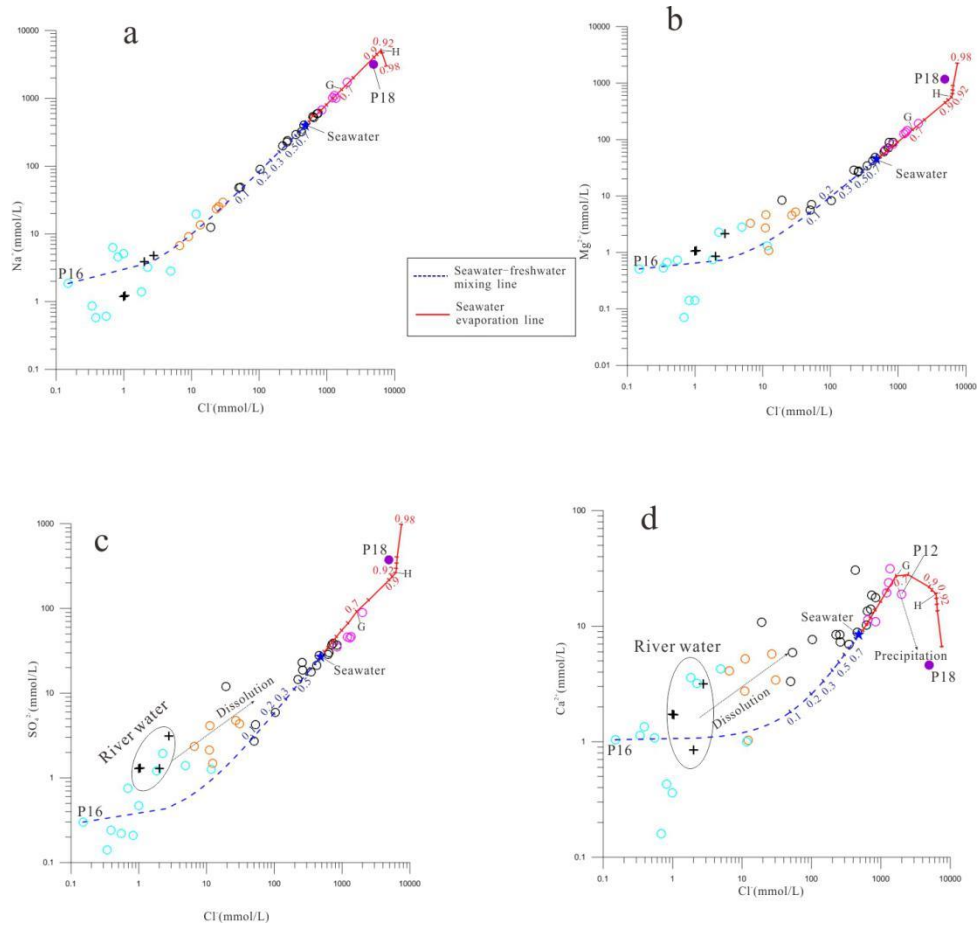
The depletion of ¹⁸O and ²H values in the deep fresh groundwater (Fig. 4) can be attributed to a cold climate (Kreuzer et al., 2009) and residence time of P15-150 and P14-300 samples (range from 33951 to 39050 a B.P) which may suggest that there was a recharge during the last glacial maximum. The stable isotopes of P16-100 are more heavier, reflecting the recharge history of warm climate in the previous deglaciation (Hendry and Wassenaar, 2000). The stable isotope values of river samples are similar to those of the shallow brackish and fresh groundwater compositions of the approximate

1 modern age, indicating lateral recharge of surface water locally. Meanwhile, in Fig. 4,
2 G03-5 is close to the rainfall sample, indicating that modern precipitation is a new
3 recharge source. The trend toward $\delta^{2}\text{H}$ and $\delta^{18}\text{O}$ enrichment in brine and saline
4 groundwater could be attributed to seawater infiltration during Holocene transgression
5 period, which has been confirmed by other study in Bohai Sea coast (Li et al., 2017, Du
6 et al., 2016). Additionally, due to the mixing of meteoric water and the subsequent non-
7 equilibrium fractionation of hydrogen isotope during evaporation (Clark and Fritz,
8 1997), the CSW sample is characterized by ^{18}O enrichment compared to seawater but
9 ^{2}H depletion.

10 5.2 Hydrochemical analysis for sources of salinity

11 For distinguishing the sources of groundwater salinity, the PHREEQC code
12 (Parkhurst and Appelo, 2013) was used to measure and plot the theoretical seawater-
13 freshwater mixing line (“mixing line”) and seawater evaporation line (“evaporation
14 line”) using hydrogeochemical modeling. Using both simulation effects as references
15 to groundwater hydrochemical characteristics (Figs. 6 and 7. For the Na-Cl (Fig. 6a),
16 Mg-Cl (Fig. 6b), and Br-Cl (Fig. 7a) diagrams, whose measured brackish, saline and
17 brine groundwater samples fit quite well to modeling mixing lines, and evaporation
18 lines follow linear trends from the least to the most saline. This would strongly
19 demonstrate that, the salt in these water samples is mainly of marine origin. The major
20 ions concentration in some samples (such as brine) is higher than those in the seawater,
21 suggesting the enriched ions are associated with evaporation processes rather than
22 seawater intrusion (Colombani et al, 2017).

1 Moreover, the samples deviate from the modeling lines (Fig. 6c and 6d), indicating
2 that there may be other hydrogeochemical processes responsible for the modified ionic
3 compositions (Giambastiani et al., 2013): (1) Ca^{2+} depletion of P18 and P12 samples
4 are shown in Fig. 6d. This phenomenon is likely explained by gypsum (CaSO_4)
5 precipitation. The evaporation line reveals that the Ca^{2+} composition of evaporating
6 seawater follows a hooked trajectory (Fig. 6d). During evaporation to the point of
7 gypsum saturation, residual CSW becomes progressively decreased Ca^{2+} concentration.
8 (2) Ca^{2+} and SO_4^{2-} excess in most fresh and brackish samples (Fig. 6c and d) could be
9 attributed to mineral dissolution along with stream water recharging (such as gypsum
10 dissolution), highlighting some degree of dilution with continental runoff since
11 Holocene regression. (3) Decomposition of organic matters abundant in marine or
12 lagoon facies sediments can result in the release of bromide ions, thus making the Br/Cl
13 ratios of saline groundwater samples higher than the mixing line (Fig. 7b).



1

2 Fig. 6 Hydrochemical relationship between Cl and major ions of measured samples and simulated

3 results (seawater-freshwater mixing line: theoretical mixing between seawater and deep fresh

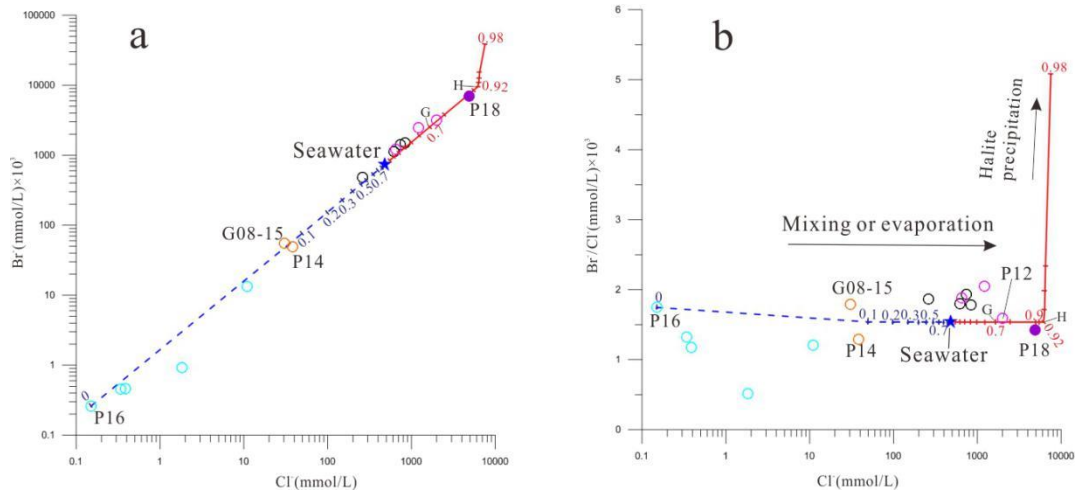
4 groundwater, and the blue numbers are mixing ratios of seawater; seawater evaporation line:

5 theoretical evaporation of Bohai seawater, and the red numbers are different evaporation rates) in

6 groundwater. G and H stand for point of precipitation of gypsum, halite respectively. The

7 “Dissolution” represents possible gypsum dissolution along with river water recharging. The

8 symbols of samples are same as Fig. 6.



1

2 Fig. 7 Relationship between chloride and bromide content in water samples. Symbols are same as

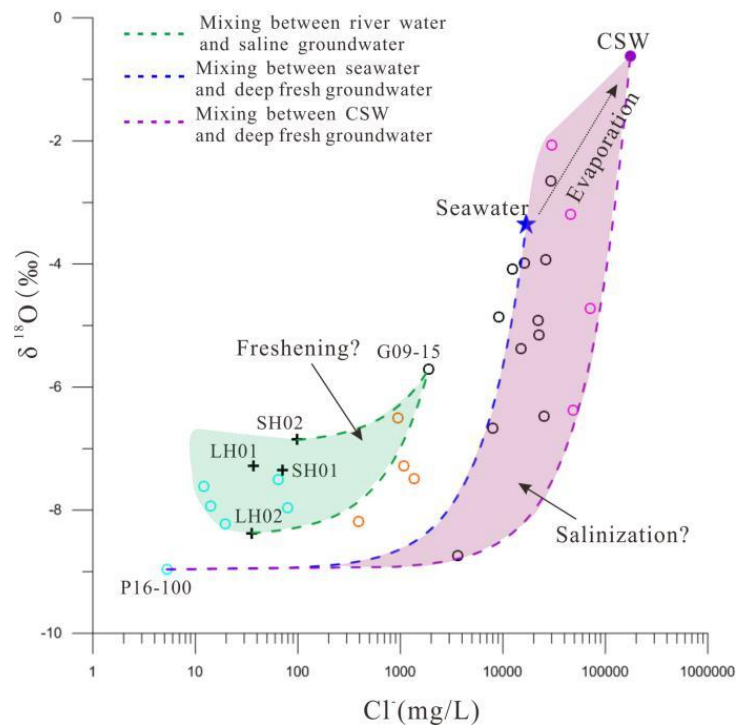
3

Fig. 6.

4 5.3 Mixing processes

5 Fig. 8 depicts the relationship between $\delta^{18}\text{O}$ and Cl^- in different water samples. There
 6 is a higher Cl^- concentration and lighter $\delta^{18}\text{O}$ values in brine samples than in seawater,
 7 meaning that simple two end-members mixing cannot adequately explain groundwater
 8 salinization. Stable isotopes of high TDS saline and brine samples fall between the
 9 seawater and CWS mixing lines, suggesting potential three end-member mixing
 10 processes (Douglas et al., 2000). Therefore, we considered SW01 (seawater) and P18
 11 (most saline but with relatively depleted stable isotope) as two saline end-members.
 12 The P16-100, which is most likely recharged during the Last Deglaciation, was chosen
 13 to represent fresh end-members that could have been impacted by overlying seawater
 14 or CSW during Holocene transgression. In Fig. 8, an inferred salinization zone was
 15 established that included almost all saline and brine groundwater samples,
 16 demonstrating the salinization processes in which fresh groundwater mixed with either
 17 seawater, CSW, or a mixture of both.

1 The fresh and brackish groundwater samples, on the other hand, have low Cl^-
 2 concentrations and lighter ^{18}O , deviating from the assumed salinization zone but
 3 approaching the river samples in Fig. 8, implying a river water-groundwater mixing
 4 trend. The LH02 (lighter $\delta^{18}\text{O}$) and SH02 (relatively heavier $\delta^{18}\text{O}$) were selected to
 5 represent river water end-members range for different continental runoff in study area,
 6 while the G09-15 (saline but with river-like stable isotope) was considered as a
 7 groundwater end-member. There is a presumed freshening zone could form between
 8 two river water-groundwater mixing lines, indicating occurrence of freshening
 9 processes which would be in agreement with continental runoff dilution discussed in
 10 section 5.2.



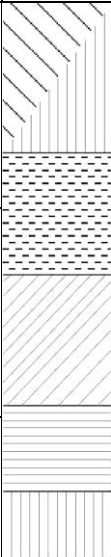

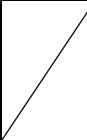


11
 12 Fig. 8 Relationship between Cl and $\delta^{18}\text{O}$ of different water samples as means to various mixing
 13 processes in the Luanhe River Delta. The symbols are same as Fig. 6. The green area is assumed
 14 freshening zone, and the purple area is assumed salinization zone.

1 **6 Interpretation of palaeo-environmental development**

2 Based on analysis of a range of evidence related to Quaternary geographic evolution,
3 it is possible to understand the change of hydrogeological conditions in the past (Van
4 Engelen et al., 2018). The Pleistocene transgression events-related to Marine isotope
5 stage (MIS) 3 and 5-have been observed to reach the study area by other authors once
6 (Wang et al., 1981; Peng et al., 1981; Li et al., 1982; Li et al., 1983; Xu et al., 2018,),
7 which would be resulted in groundwater salinization. Since the last deglaciation (about
8 15 ka B.P.), the palaeo-coast line has approximately 100 m depth below present sea
9 level along the shelf edge (Li et al., 2014). Stronger river down-cutting and flushing in
10 the study region would have been helped a large fresh recharge of groundwater. For
11 example, P16-100 (fresh water) was sampled from a relatively deep position (100 m
12 below surface) has an estimated groundwater age between 15959 to 17490 a B.P., which
13 is likely to provide evidence that the salinization groundwater related to MIS 5 and/or
14 3 marine transgression could have been flushed out until the Latest Pleistocene.
15 Accordingly, we believe that the observed saline groundwater in the Luanhe River Delta
16 is probably related to the subsequent Holocene marine transgression. This research
17 develops the evolutionary pattern of saline groundwater, as shown in Table 1 and Fig.
18 Three phases are synthesized and reconstructed.

19

1 Table 1 Saline groundwater evolution processes in study area

Evolution stage	Groundwater evolution processes		Influencing factors			Major Hydrogeochemical processes	Sediments	
	Evolution pattern	Factors	Palaeoclimate	Geological setting	Others			
Phase 3 The development of new delta (3.5 ka B.P. to present)	Freshening	Wash-out of surface water	Temperate, slightly semi-humid	Development of surface stream	Irrigation return	Mixing and leaching		Holocene alluvial deposit or artificial fill Bottom sediments age about 1795—302 a B. P. (Xu et al., 2020 He et al., 2020)
	Deceleration of brine formation	Limitation of seawater evaporation		Diversion of channels and lagoon filled by diluvial deposit	Artificial reclamation and offshore levees			Holocene lagoon facies Bottom sediments age about 5995—1600 a B. P. (Cheng et al., 2020 He et al., 2020)
Phase 2 The development of old delta (7 to 3.5 ka B.P.)	Brine formation	Seawater evaporation and CSW infiltrating	Temperate, slightly arid	Deceleration of sea-level rising, development of delta, and coastal lagoons have been active	Tides or storm	Mixing, leaching, evaporation, and mineral precipitation		Holocene delta facies Bottom sediments age about 6675—3695 a B. P. (He et al., 2020)
Phase 1 Holocene transgression (12to 7 ka B.P.)	Groundwater salinization	Palaeo-seawater intrusion	Temperate -warm, humid	Deglaciation of ice sheet, rapid rising of sea level, Holocene transgression		Mixing		Holocene marine facies Bottom sediments age about 8620—5595 a B. P. (Li et al., 1982)
								Late Pleistocene continental facies (Xu et al., 2020 He et al., 2020)

2 *Phase 1: Transgressive system tract-Holocene transgression stage (9-7 ka B.P.)*

3 Global sea level was affected by deglaciation of the ice sheet (Fairbanks, 1989),
 4 causing sea level to rise rapidly during the deglaciation period (15.4-7 ka B.P.) (Li et
 5 al., 2014). It could be summarized that the Holocene transgression stage, which
 6 occurred between 9 and 7 ka B.P, resulted in the study area being inundated by seawater
 7 (Xu et al., 2015; Xue 2009, 2014) (Fig. 9a). On the one hand, there would have been a
 8 tendency for the denser seawater to infiltrate through the aeration zone (Santucci et al.,
 9 2016); on the other hand, sea-level rise would cause the seawater-freshwater interface
 10 to move landward (Ferguson and Gleeson, 2012), both of which contributed to palaeo-
 11 seawater intrusion. The G08-40 contains TDS of 27.173 g/L, which is more similar to
 12 that of SW01. Simultaneously, the residence time (9810-6884 a B.P.) indicates trapped
 13 palaeo-seawater at low-permeability aquitard sediments still exists and may be another
 14 critical salinity source for neighboring aquifers in the coastal zone (Post and Kooi, 2003;

1 Lee et al., 2016).

2 The presence of palaeo-seawater intrusion during Quaternary has been recorded in
3 other coastal regions worldwide (Groen et al., 2000; Bouchaou et al., 2009; Wang and
4 Jiao, 2012; Delsman et al., 2014; Tran et al., 2020; Han et al., 2020). For the works
5 described above, the salinity of groundwater after salinization could not exceed that of
6 seawater due to palaeo-seawater intrusion.

7 Other salinization processes that occurred during palaeo-environmental growth are
8 likely to be correlated with such brine groundwater.

9 *Phase 2: Highstand system tract-Old Luanhe River Delta development (7-3.5 ka B.P.)*

10 The good fit between the measured hydrochemistry and simulated evaporation lines
11 (Fig. 6 and 7) is an indicator that the brine samples were associated with the seawater
12 which was exposed to evaporation during geological history. Previous research has
13 revealed that lagoon was active during the progradation of the old Luanhe River Delta
14 between 7 and 3.5 ka B.P. (He et al., 2020; Xu et al., 2020). Meanwhile, the relatively
15 arid climate had been developed since 5500 a B.P., which may lead to increased
16 evaporation (Jin, 1984). The ancient lagoon would be an ideal location for evaporating
17 seawater that had been trapped due to storms or tides (Fig. 9b). As a result, concentrated
18 saline water (CSW) with salinity heavier than seawater would have created, and the
19 CSW would go through two processes: (1) infiltrating and descending to the lower part
20 of the aquifer due to its higher density, and combining with the salinized groundwater
21 from phase 1, resulting in a three end-members mixing scenario in the relationship
22 diagram (Fig. 8). (2) After reaching saturation during the later stages of evaporation,

1 mineral precipitation, such as gypsum, calcite, and halite, would occur, and this would
2 be subjected to redissolution by meteoric waters or seawater, resulting in high salinity
3 water that would then be subjected to the above process; The Br/Cl ratios in certain
4 fresh or brine groundwater samples deviate from the evaporation line (Fig. 7b), which
5 may be related to halite precipitation and redissolution. These two processes caused
6 groundwater salinity to rise even further, resulting in the formation of brine
7 groundwater with 3 times the TDS of seawater, such as G03-20 with a range of resident
8 time of 4323 to 5590 a B.P.

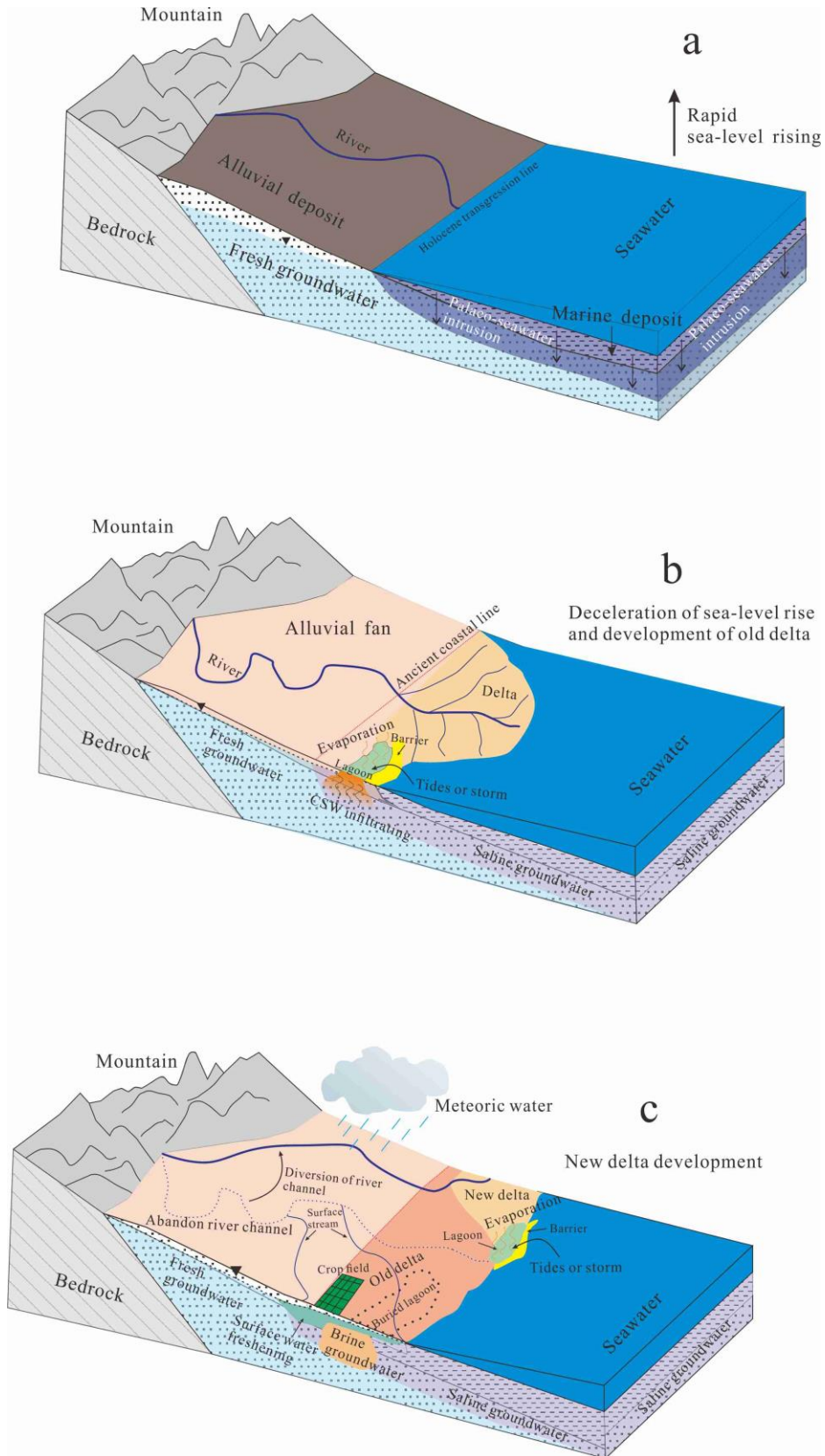
9 *Phase 3: New Luanhe River Delta development (3.5 ka B.P. -present)*

10 Since about 3500 a B.P., a nearly 90-degree diversion of the Luanhe River channel
11 in the study area resulted in new delta development (Wang et al., 2007; Xue, 2016).
12 There are some signs of a lagoon environment in the new Luanhe River Delta (Cheng
13 et al., 2020), and, as previously discussed, the brine groundwater sample G10-30 would
14 be attributed to evaporation in a lagoon setting (Fig. 9c). However, some factors are
15 likely to limit the CSW formation in the study area: (1) the relatively low evaporation
16 capacity due to semi-humid climate since about 2.5 ka B.P. (Jin, 1984), (2) the diluvial
17 deposit or artificial reclamation would have filled the coastal lowland such as lagoons,
18 and (3) offshore levees prevent the seawater from flooding inland during storms or tides.
19 Unlike the old Luanhe River Delta, these factors may also explain why the current
20 Luanhe River Delta does not have high TDS brine groundwater.

21 In addition, the brackish and low TDS saline groundwater with relatively modern age
22 (e.g. G09-15), and river-like stable isotopes (Fig. 4 and 8), are compelling evidence that

1 freshening processes have occurred in the delta plain. Since the semi-humid
2 palaeoclimate, some abandoned channels have developed into small rivers after the
3 diversion of the ancient Luanhe River (Gao, 1981), such as the Suhe River and Shahe
4 River. Firstly, the lateral recharge from the surface stream plays a role in washing out
5 the salty groundwater. Secondly, due to the inefficiency of saline groundwater
6 throughout human history, river irrigation has been commonly used for agricultural
7 activities in the study region, freshening the upper saline aquifer (Fig. 9c). Some
8 groundwater samples found above the seawater mixing line in the Ca-Cl and SO₄-Cl
9 relationship diagrams (Fig. 6c, d) may be related to mineral dissolution during river
10 water or irrigation recharge. However, saline groundwater can be washed out over time
11 in coastal zones with low-permeable marine layers and a low hydraulic gradient (van
12 Engelen et al., 2019; Han et al., 2020).

13 In summary, the evolution of saline groundwater in the study area results from
14 palaeo-environment development such as sea-level change, palaeogeography, and
15 palaeoclimate, and is significantly affected by human activities. The coastal brine
16 groundwater is a special product of geological evolution, which have been found in
17 Bohai Sea coast such as Bohai Bay (Li et al., 2017) and Laizhou Bay (Han et al., 2014).
18 The change in sea level over the Late Pleistocene would have favoured marine intrusion
19 and similar sedimentary environment in Bohai coast, allowing this study infers the
20 following conditions for its brine formation: (1) stable evaporative environments (e.g.
21 lagoon), (2) suitable climatic conditions (e.g. arid), (3) seawater entering evaporative
22 environments (e.g. storm or tide), and (4) long-term scale for salinity accumulation.



1

2 Fig. 9 Diagram of palaeoenvironmental development since Holocene and evolutionary pattern of

3

saline groundwater.

1 **7 Conclusions**

2 In this study, we used a range of isotopic-geochemical methods to analyze
3 groundwater's recharge and salinity source in the Luanhe River Delta. The isotopic
4 results (^2H , ^{18}O , ^{14}C) show that deep confined groundwater was recharged during the
5 Late Pleistocene cold period, shallow saline and brine groundwater was recharged
6 during the warm Holocene period, and shallow brackish and fresh groundwater was
7 mainly recharged by surface water. The hydrogeochemical modeling (PHREEQC)
8 results show that seawater or evaporated seawater is the primary salty source in
9 salinized groundwater. The variation in the ^{18}O -Cl relationship of multiple water
10 samples further indicates multiple end-member mixing, which is useful to assess the
11 salinization and/or freshening processes in aquifers. Our study shows that multiple
12 water types are particularly associated with complex geographic evolution in coastal
13 areas. The variation in sea-levels (when it rises) causes lowland coastal areas to be
14 inundated by seawater, which induces palaeo-seawater intrusion. The coastal deltas
15 developed after a significant drop in the sea levels. The concentration of saline water in
16 the lagoon environment at the delta-front continuously provided salinity to the
17 groundwater. Thus, brine groundwater was formed under the effects of evaporation,
18 mixing, and dissolution. In contrast, the lateral recharge of surface water and irrigation
19 return would cause slow wash-out of salinized groundwater in the delta plain.

20 Given that most coastal zones around the world experienced transgression/regression
21 events in the Quaternary period, this work's findings will promote a better
22 understanding of the origin of salinization in coastal aquifers. In addition, it is important

1 to recognize the potential leak of connate saline groundwater previously preserved in
2 adjunct aquifers that can occur due to the over-extraction of deep groundwater. To
3 effectively prevent pollution from saline groundwater movement, this study
4 recommends extensive characterization of groundwater interface dynamics, such as
5 fresh/saline, fresh/brine, and brine/seawater interfaces, and also maintain continuous
6 monitoring of water quality and levels across the aquifers
7

1 **Data availability**

2 The data used in this paper are available in the Supplement.

3

1 **Authors contribution**

2 Xianzhang Dang: Conceptualization, Formal analysis, Investigation, Writing-Original

3 Draft, Data curation.

4 Maosheng Gao: Funding acquisition, Methodology, Supervision, Investigation,

5 Writing-Review & Editing.

6 Zhang Wen: Supervision, Writing-Review & Editing.

7 Guohua Hou: Project administration, Investigation.

8 Hamza Jakada: Writing-Review & Editing.

9 Daniel Ayejoto: Writing-Review & Editing.

10 Qiming Sun: Investigation.

11

1 **Competing interests**

2 The authors declare that they have no conflict of interest.

3

1 **Acknowledgement**

2 This study was financially supported by the National Natural Science Foundation of
3 China (U2106203, 41977173), National Geological Survey Project of China Geology
4 Survey (No. DD20211401) and China-ASEAN maritime cooperation fund
5 (Comparative Study of Geoenvironment and Geohazards in the Yangtze River Delta
6 and the Red River Delta). The authors would like to thank Sen Liu, Chenxin Feng, Chen
7 Sheng, Xueyong Huang and Haihai Zhuang, for their help and support in collecting
8 field data and conducting geological survey.

1 **References**

2 Akouvi, A., Dray, M., Violette S., de Marsily, G., and Zuppi G. M.: The sedimentary
3 coastal basin of Togo: example of a multilayered aquifer still influenced by a
4 palaeo-seawater intrusion, *HYDROGEOL J*, 16, 419-436,
5 <https://doi.org/10.1007/s10040-007-0246-1>, 2008.

6 Aquilina, L., Vergnaud-Ayraud, V., Les Landes, A. A., Pauwels, H., Davy, P., Petelet-
7 Giraud, E., Labasque, T., Roques, C., Chatton, E., and Bour, O.: Impact of climate
8 changes during the last 5 million years on groundwater in basement aquifers, *SCI*
9 *REP-UK*, 5, 14132, <https://doi.org/10.1038/srep14132>, 2015.

10 Bouchaou, L., Michelot, J. L., Qurtobi, M., Zine, N., Gaye, C. B., Aggarwal, P. K.,
11 Marah H., Zerouali, A., Taleb, H., and Vengosh, A.: Origin and residence time of
12 groundwater in the Tadla basin (Morocco) using multiple isotopic and
13 geochemical tools, *J HYDROL*, 379, 323-338,
14 <https://doi.org/10.1016/j.jhydrol.2009.10.019>, 2009.

15 Cary, L., Petelet-Giraud E., Bertrand G.,nKloppmann, W., Aquilina, L., Martins, V.,
16 Hirata, R., Montenegro, S., Pauwels, H., Chatton, E., Franzen, M., and Aurouet,
17 A.: Origins and processes of groundwater salinization in the urban coastal aquifers
18 of Recife (Pernambuco, Brazil): A multi-isotope approach, *SCI TOTAL*
19 *ENVIRON*, 530-531, 411-429, <https://doi.org/10.1016/j.scitotenv.2015.05.015>,
20 2015.

21 Cartwright, I., Currell, M., Cendon, D., and Meredith, K.: A review of the use of
22 radiocarbon to estimate groundwater residence times in semi-arid and arid areas,

1 J Hydrol, 580, 124247. <https://doi.org/10.1016/j.jhydrol.2019.124247>, 2020.

2 Chen, Z. Y., Qi, J. X., Xu, J. M., Xu, J. M., Ye, H., and Nan, Y. J.: Paleoclimatic
3 interpretation of the past 30 ka from isotopic studies of the deep confined aquifer
4 of the North China Plain, APPL GEOCHEM, 18, 997-1009,
5 [https://doi.org/10.1016/S0883-2927\(02\)00206-8](https://doi.org/10.1016/S0883-2927(02)00206-8), 2003.

6 Cheng, L. Y., Xu, Q. M., Guo, H., Li, M., Yang, N., Liu, J. B., Zhao, J. J., and Guo, J.
7 J.: The Late Holocene Stratum and evolution in the Luanhe River Delta,
8 Quaternary Sciences, 40 (3), 751-763,
9 <https://doi.org/10.27355/d.cnki.gtjisy.2020.000012>, 2020 (In Chinese with English
10 abstract).

11 Clark, I. D., and Fritz, P.: Environmental Isotopes in Hydrogeology, Lewis Publishers,
12 New York, 1997.

13 Colombani, N., Cuoco, E., and Mastrocicco, M.: Origin and pattern of salinization in
14 the Holocene aquifer of the southern Po Delta (NE Italy), J GEOCHEM EXPLOR,
15 175: 130-137, <https://doi.org/10.1016/j.gexplo.2017.01.011>, 2017.

16 Costall A. R., Harris B. D., Teo, B., Schaa, R., Wagner, F. M., and Pigois, J. P.:
17 Groundwater Throughflow and Seawater intrusion in High Quality coastal
18 Aquifers, SCI REP-UK, 10: 9866, <https://doi.org/10.1038/s41598-020-66516-6>,
19 2020.

20 Craig, H.: Standard for reporting concentration of deuterium and oxygen-18 in natural
21 water, SCIENCE, 133, 1833-1834, <https://doi.org/10.1126/science.133.3467.1833>,
22 1961.

1 Currell, M. J., Cartwright, I., Bradley, D. C., and Han, D. M.: Recharge history and
2 controls on groundwater quality in the Yuncheng Basin, north China, *J HYDROL*,
3 385, 216-229., <https://doi.org/10.1016/j.jhydrol.2010.02.022>, 2010.

4 Dang, X .Z., Gao, M. S., Wen, Z., Jakada, H., Hou, G. H., and Liu, S.: Evolutionary
5 process of saline groundwater influenced by palaeo-seawater trapped in coastal
6 deltas: A case study in Luanhe River Delta, China, *ESTUAR COAST SHELF S*,
7 244, 106894, <https://doi.org/10.1016/j.ecss.2020.106894>, 2020.

8 de Montety, V., Radakovitch, O., Vallet-Coulomb, C., Blavoux, B., Hermitte, D., and
9 Valles, V.: Origin of groundwater salinity and hydrogeochemical processes in a
10 confined coastal aquifer: case of the Rhone delta (Southern France), *APPL*
11 *GEOCHEM*, 23(8), 2337-2349, <https://doi.org/10.1016/j.apgeochem.2008.03.011>,
12 2008.

13 Delsman, J. R., Hu-a-ng, K. R. M., Vos, P. C., de Louw, P. G. B., Oude Essink, G. H. P.,
14 Stuyfzand, P.J., and Bierkens, M.F.P.: Paleo-modeling of coastal saltwater
15 intrusion during the Holocene: an application to the Netherlands, *HYDROL*
16 *EARTH SYST SC*, 18(10), 3891-3905, [https://doi.org/10.5194/hess-18-3891-](https://doi.org/10.5194/hess-18-3891-2014)
17 2014,2014.

18 Douglas, M., Clark, I. D., Raven, K., and Bottomley, D.: Groundwater mixing dynamics
19 at a Canadian Shield mine, *J HYDROL*, 235, 88-103,
20 [https://doi.org/10.1016/S0022-1694\(00\)00265-1](https://doi.org/10.1016/S0022-1694(00)00265-1), 2000.

21 Du, Y., Ma, T., Chen, L. Z., Shan, H. M., Xiao, C., Lu, Y., Liu, C. F., and Cai, H. S.:
22 Genesis of salinized groundwater in Quaternary aquifer system of coastal plain,

1 Laizhou Bay, China: Geochemical evidences, especially from bromine stable
2 isotope, APPL GEOCHEM, 2015, 59:155-165,
3 <https://doi.org/10.1016/j.apgeochem.2015.04.017>, 2015.

4 Du, Y., Ma, T., Chen L., Xiao, C., and Liu, C. F.: Chlorine isotopic constraint on
5 contrastive genesis of representative coastal and inland shallow brine in China, J
6 GEOCHEM EXPLOR, 170 (2016): 21-29,
7 <https://doi.org/10.1016/j.gexplo.2016.07.024>, 2016.

8 Edmunds, W. M.: Palaeowaters in European coastal aquifers-the goals and main
9 conclusions of the PALAEAUX project, Geological Society London Special
10 Publications, 189, 1-16, <https://doi.org/10.1144/GSL.SP.2001.189.01.02>, 2001.

11 Fairbanks, R. G.: A 17,000-year glacio-eustatic sea level record: influence of glacial
12 melting rates on the Younger Dryas event and deep ocean circulation, NATURE,
13 342, 637-647, <https://doi.org/10.1038/342637a0>, 1989.

14 Feng, J. and Zhang, W.: The evolution of the modern Luanhe River delta, north China,
15 GEOMORPHOLOGY, 25 (3), 269-278, [https://doi.org/10.1016/S0169-555X\(98\)00066-X](https://doi.org/10.1016/S0169-555X(98)00066-X), 1998.

16

17 Ferguson, G., and Gleeson, T.: Vulnerability of coastal aquifers to groundwater use and
18 climate change, NAT CLIM CHANGE, 2, 342-345,
19 <https://doi.org/10.1038/nclimate1413>, 2012.

20 Fontes, J. C., and Garnier, J. M.: Determination of the initial ¹⁴C activity of the total
21 dissolved carbon: a review of the existing models and a new approach. WATER
22 RESOUR RES, 15 (2), 399-413, <https://doi.org/10.1029/wr015i002p00399>,

1 1979.

2 Gao, S. M.: Facies and sedimentary model of the Luan River delta. *Acta Geographica*
3 *Sinica*, 48 (3), 303-314, 1981 (in Chinese with English abstract).

4 Giambastiani, B. M. S., Colombani, N., Mastrocicco, M. and Fidelibus, M. D.:
5 Characterization of the lowland coastal aquifer of Comacchio (Ferrara, Italy):
6 Hydrology, hydrochemistry and evolution of the system, *J HYDROL*, 501: 35-44,
7 <https://doi.org/10.1016/j.jhydrol.2013.07.037>, 2013.

8 Gibson, J. J., Edwards, T. W., Burse, G. G., and Prowse, T. D.: Estimating evaporation
9 using stable isotopes: quantitative results and sensitivity analysis for two
10 catchments in Northern Canada, *Nordic Hydrology*. 24, 79-94,
11 <https://doi.org/10.2166/nh.1993.0015>, 1993.

12 Groen, J., Velstra, J., and Meesters, A.: Salinization processes in paleowaters in coastal
13 sediments of Suriname: evidence from $\delta^{37}\text{Cl}$ analysis and diffusion modelling, *J*
14 *HYDROL*, 234, 1-20, [https://doi.org/10.1016/S0022-1694\(00\)00235-3](https://doi.org/10.1016/S0022-1694(00)00235-3), 2000.

15 Han, D. M., Kohfahl, C., Song, X. F., Xiao G. Q., and Yang, J. L.: Geochemical and
16 isotopic evidence for Palaeo-Seawater intrusion into the south coast aquifer of
17 Laizhou Bay, China, *APPL GEOCHEM*, 26 (5), 863-883,
18 <https://doi.org/10.1016/j.apgeochem.2011.02.007>, 2011.

19 Han, D. M., Song, X. F., Currell, M. J., Yang, J. L., and Xiao G. Q.: Chemical and
20 isotopic constraints on the evolution of groundwater salinization in the coastal
21 plain aquifer of Laizhou Bay, China, *J HYDROL*, 508, 12-27,
22 <https://doi.org/10.1016/j.jhydrol.2013.10.040>, 2014.

- 1 Han, D. M., and Currell, M. J.: Delineating multiple salinization processes in a coastal
2 plain aquifer, northern China: hydrochemical and isotopic evidence, *HYDROL*
3 *EARTH SYST SC*, 22, 3473-3491, <https://doi.org/10.5194/hess-22-3473-2018>,
4 2018.
- 5 Han, D. M., Cao G. L., Currell, M. J., Priestley, S. C., and Love, A. J.: Groundwater
6 salinization and flushing during glacial-interglacial cycles: insights from aquitard
7 porewater tracer profiles in the North China Plain, China, *WATER RESOUR RES*,
8 56 (11), <https://doi.org/10.1029/2020WR027879>, 2020.
- 9 He L., Amorosi A., Ye S. Y., Xue, C. T., Yang, S. X., and Laws E.A.: River avulsions
10 and sedimentary evolution of the Luanhe fan-delta system (North China) since the
11 late Pleistocene, *MAR GEOL*, 425,106194,
12 <https://doi.org/10.1016/j.margeo.2020.106194>, 2020.
- 13 Hendry, M. J. and Wassenaar, L. I.: Controls on the distribution of major ions in pore
14 waters of thick surficial aquitard, *WATER RESOUR RES*, 36 (2), 503-513,
15 <https://doi.org/10.1029/1999WR900310>, 2000.
- 16 IAEA/WMO: Global Network of Isotopes in Precipitation, The GNIP Database, Vienna,
17 available at: http://www-naweb.iaea.org/napc/ih/IHS_resources_gnip.html (last
18 access: 18 November 2013), 2006.
- 19 Jayathunga K., Diyabalanage S., Frank A. H., Chandrajith, R., and Barth, J. A. C.:
20 Influences of seawater intrusion and anthropogenic activities on shallow coastal
21 aquifers in Sri Lanka: evidence from hydrogeochemical and stable isotope data,
22 *ENVIRON SCI POLLUT R*, 2020, 27(18), <https://doi.org/10.1007/s11356-020->

1 08759-4, 2020.

2 Jiao, J. J. and Post, V.: Coastal Hydrology, Cambridge University Press, New York,
3 2019.

4 Jin, X. F.: The spore-pollen assemblages and the stratigraphy and palaeogeography in
5 western Bohai Sea since late Pleistocene, Marine Science Bullition 3, 16-24, 1984
6 (in Chinese with English abstract).

7 Kooi, H., Groen, J., and Leijnse, A.: Modes of seawater intrusion during transgressions,
8 WATER RESOUR RES, 36, 3581–3589, <https://doi.org/10.1029/2000wr900243>,
9 2000.

10 Kreuzer, A. M., Rohden, C. V., Friedrich, R., Chen, Z. Y., Shi, J. S., Hajdas, I., Kipfer,
11 R., and Aeschbach-Hertig, W.: A record of temperature and monsoon intensity
12 over the past 40 kyr from groundwater in the North China Plain, CHEM GEOL,
13 259, 168-180, <https://doi.org/10.1016/j.chemgeo.2008.11.001>, 2009.

14 Larsen, F., Tran, L. V., Van Hoang, H., Tran, L. T., Christiansen, A. V., and Phan, N.Q.:
15 Groundwater salinity influenced by Holocene seawater trapped in incised valleys
16 in the Red River delta. NAT GEOSCI, 10, 376-381,
17 <https://doi.org/10.1038/ngeo2938>, 2017.

18 Lee, S., Currell, M., and Cendon, D. I.: Marine water from mid-Holocene sea level
19 highstand trapped in a coastal aquifer: Evidence from groundwater isotopes, and
20 environmental significance, SCI TOTAL ENVIRON, 544, 995-1007,
21 <https://doi.org/10.1016/j.scitotenv.2015.12.014>,2016.

22 Li, G. X., Li, P., Liu, Y., Qiao, L. L., Ma, Y. Y., Xu, J. S., and Yang, Z. G.: Sedimentary

- 1 system response to the global sea level change in the East China Seas since the
2 last glacial maximum, *EARTH-SCI REV*, 139 (2014), 390-405,
3 <https://doi.org/10.1016/j.earscirev.2014.09.007>, 2014.
- 4 Li, H. M. and Wang, J. D.: Palaeomagnetic study on drill core from northern Bohai
5 coastal plain. *Geochimica*, 2, 196-204, 1983 (in Chinese with English abstract).
- 6 Li, J., Liang, X., Jin, M. G., and Mao X. M.: Geochemical signature of aquitard pore
7 water and its paleo-environment implications in Caofeidian Harbor, China,
8 *GEOCHEM J*, 47, 37-50, <https://doi.org/10.2343/geochemj.2.0238>, 2013.
- 9 Li, Y. F., Gao, S. M. and An, F. T.: A preliminary study of the Quaternary marine strata
10 and its paleogeographic significance in the Luanhe delta region, *Oceanologia et*
11 *Limnologia Sinica*, 13 (5), 433-439, 1982 (in Chinese with English abstract).
- 12 Liu, S., Tang, Z. H., Gao, M. S., and Hou, G.H.: Evolutionary process of saline-water
13 intrusion in Holocene and Late Pleistocene groundwater in southern Laizhou Bay,
14 *SCI TOTAL ENVIRON*, 607-608, 586-599,
15 <https://doi.org/10.1016/j.scitotenv.2017.06.262>, 2017.
- 16 Ma, F. S., Wei, A. H., Deng, Q. H., and Zhao H. J.: Hydrochemical Characteristics and
17 the Suitability of Groundwater in the Coastal Region of Tangshan, China, *J*
18 *EARTH SCI-CHINA*, 26 (6), 1067-1075, [https://doi.org/10.1007/s12583-014-](https://doi.org/10.1007/s12583-014-0492-9)
19 [0492-9](https://doi.org/10.1007/s12583-014-0492-9), 2014.
- 20 Niu, Z. X., Jiang X. W. and Hu, Y. Z.: Characteristics and causes of hydrochemical
21 evolution of deep groundwater in the Luanhe delta, *Hydrogeology and*
22 *Engineering Geology*, 46 (01), 27-34, 2019 (in Chinese with English abstract).
- 23 Parkhurst, D. L., Appelo, C. A. J.: Description of input and examples for PHREEQC

- 1 version 3-a computer program for speciation, batch-reaction, one-dimensional
2 transport, and inverse geochemical calculations, U.S. Geological Survey
3 Techniques and Methods, book 6, chap. A43, 497 pp., available only at
4 <http://pubs.usgs.gov/tm/06/a43/>, 2013.
- 5 Peng, G., Jiao, W. Q., Li, D. M., and Li, G. Y.: Division and correlation of the late
6 Quaternary stratigraphy and discussion on the recent tectonic movement in the
7 region of the Luanhe River Delta, *Seismology and Geology*, 3, 31-36, 1981 (in
8 Chinese with English abstract).
- 9 Pearson, F. J. and Hanshaw, B. B.: Sources of dissolved carbonate species
10 ingroundwater and their effects on carbon-14 dating. In: IAEA (Ed.), *Isotope
11 Hydrology*, IAEA, Vienna, 1970.
- 12 Post, V. E. and Kooi, H.: Rates of salinization by free convection in high-permeability
13 sediments: insight from numerical modeling and application to Dutch coastal area,
14 *HYDROGEOLOGICAL JOURNAL*, 11, 549-559, <https://doi.org/10.1007/s10040-003-0271-7>, 2003.
- 15 Qi, H. H., Ma, C. M., He, Z. K., Hu X. J., and Gao, L.: Lithium and its isotopes as
16 tracers of groundwater salinization: A study in the southern coastal plain of
17 Laizhou Bay, China, *SCI TOTAL ENVIRON*, 650:878-890,
18 <https://doi.org/10.1016/j.scitotenv.2018.09.122>, 2019.
- 19 Reilly, T. E. and Goodman, A. S.: Quantitative analysis of saltwater-freshwater
20 relationships in groundwater systems-a historical perspective, *J HYDROL*, 80,
21 125-160, [https://doi.org/10.1016/0022-1694\(85\)90078-2](https://doi.org/10.1016/0022-1694(85)90078-2), 1985.
- 22 Sanford, W. E.: Groundwater hydrology: Coastal flow, *NAT GEOSCI*, 3, 671-672,

1 <https://doi.org/10.1038/ngeo958>, 2010.

2 Santucci, L., Carol, E., and Kruse E.: Identification of palaeo-seawater intrusion in
3 groundwater using minor ions in a semi-confined aquifer of the Río de la Plata
4 littoral (Argentina), *SCI TOTAL ENVIRON*, 566-567, 1640-1648,
5 <https://doi.org/10.1016/j.scitotenv.2016.06.066>, 2016.

6 Sola F., Vallejos A., Daniele L., and Pulido-Bosch A.: Identification of a Holocene
7 aquifer-lagoon system using hydrogeochemical data, *QUATERNARY RES*,
8 82,121-131, <https://doi.org/10.1016/j.yqres.2014.04.012>, 2014.

9 Stumpp, C., Ekdal, A., Gonenc, I. E. and Maloszewski, P.: Hydrological dynamics of
10 water sources in a Mediterranean lagoon, *HYDROL EARTH SYST. SC*, 18, 4825-
11 4837, <https://doi.org/10.5194/hess-18-4825-2014>, 2014.

12 Tulipano, L., Fidelibus, M. D., Panagopoulos, A.: *COST ACTION 621 Final Report*,
13 *Groundwater Management of Coastal Karstic Aquifers*, Office for the Official
14 Publications of European Community, Luxembourg, Vol. II, 366pp., ISBN 92-
15 894-0015-1, 2005.

16 Tran, D. A., Tsujimura M., Vo L. P., Nguyen, V. T., Kambuku, D., and Dang T. D.:
17 Hydrogeochemical characteristics of a multi-layered coastal aquifer system in the
18 Mekong Delta, Vietnam, *ENVIRON GEOCHEM HLTH*, 42, 661-680,
19 <https://doi.org/10.1007/s10653-019-00400-9>, 2020.

20 UN Atlas: 44 Percent of us Live in Coastal Areas, available at:
21 <http://coastalchallenges.com/2010/01/31/un-atlas-60-of-us-live-in-the-coastal->
22 areas, 2010.

- 1 Vallejos A., Sola F., Yechieli Y., and Pulido-Bosch, A.: Influence of the paleogeographic
2 evolution on the groundwater salinity in a coastal aquifer. Cabo de Gata aquifer,
3 SE Spain. J HYDROL, 557,55-66, <https://doi.org/10.1016/j.jhydrol.2017.12.027>,
4 2018.
- 5 van Engelen J., Oude Essink, G. H. P., Kooi, H., and Bierkens, M. F. P.: On the origins
6 of hypersaline groundwater in the Nile Delta aquifer, J HYDROL, 560, 301-317,
7 <https://doi.org/10.1016/j.jhydrol.2018.03.029>, 2018.
- 8 van Engelen J., Verkaik J., King J., Nofal E. R., Bierkens, M. F. P., and Oude Essink,
9 G. H. P.: A three-dimensional palaeohydrogeological reconstruction of the
10 groundwater salinity distribution in the Nile Delta Aquifer, HYDROL EARTH
11 SYST SC, 23, 5175-5198, <https://doi.org/10.5194/hess-23-5175-2019>, 2019.
- 12 Wang, P. X., Min, Q. B., Bian, Y. H., and Cheng, X. R.: Strata of Quaternary
13 transgressions in east China: A preliminary study. Acta Geologica Sinica, 1981
14 (01), 1-13, 1981 (in Chinese with English abstract).
- 15 Wang, Y. and Jiao, J. J.: Origin of groundwater salinity and hydrogeochemical processes
16 in the confined Quaternary aquifer of the Pearl River Delta, China, J HYDROL,
17 438-439, 112-124, <https://doi.org/10.1016/j.jhydrol.2012.03.008>, 2012.
- 18 Wang, Y., Fu, G., and Zhang, Y.: River-sea interactive sedimentation and plain
19 morphological evolution, Quaternary Science, 27, 674-689,
20 <https://doi.org/10.3321/j.issn:1001-7410.2007.05.009>, 2007(in Chinese with
21 English abstract).
- 22 Werner, A. D.: A review of seawater intrusion and its management in Australia,

1 HYDROGEOLOG J, 18, 281-285, <https://doi.org/10.1007/s10040-009-0465-8>, 2010.

2 Werner, A. D., Bakker, M., and Post, V. E. A., et al.: Seawater intrusion processes,
3 investigation and management: Recent advances and future challenges, ADV
4 WATER RESOUR, 51, 3-26, <https://doi.org/10.1016/j.advwatres.2012.03.004>,
5 2013.

6 Xu, Q. M., Yuan, G. B., Zhang, J. Q., Qin, Y. F.: Stratigraphic division of the Late
7 Quaternary strata along the coast of Bohai bay and its geology significance, Acta
8 Geologica Sinica, 85 (8), 1352-1367, 2011 (in Chinese with English abstract).

9 Xu, Q. M., Yang, J. L., Yuan, G. B., Chu, Z. X., and Zhang, Z. K.: Stratigraphic
10 sequence and episodes of the ancient Huanghe Delta along the southwestern Bohai
11 Bay since the LGM, MAR GEOL, 367, 69-82,
12 <https://doi.org/10.1016/j.margeo.2015.05.008>, 2015.

13 Xu, Q. M., Yang, J. L., Hu, Y. Z., Yuan, G. B., and Deng, C. L.: Magnetostratigraphy
14 of two deep boreholes in the southwestern Bohai Bay: its tectonic implications and
15 constraints on ages of volcanic layers, QUAT GEOCHRONOL, 43, 102-114,
16 <https://doi.org/10.1016/j.quageo.2017.08.006>, 2018.

17 Xu, Q. M., Meng, L. S., Yuan, G. B., Teng F., Xin H. T., and Sun X. M.: Transgressive
18 wave-and tide-dominated barrier-lagoon system and sea-level rise since 8.2 ka
19 recorded in sediments in northern Bohai Bay, China, GEOMORPHOLOGY, 352,
20 106978, <https://doi.org/10.1016/j.geomorph.2019.106978>, 2020.

21 Xue, C. T.: Historical changes of coastlines on west and south coasts of Bohai Sea since
22 7000 a B.P.. Scientia Geographica Sinica, 29, 217-222,

1 <https://doi.org/10.3969/j.issn.1000-0690.2009.02.012>, 2009 (in Chinese with
2 English abstract).

3 Xue, C. T.: Missing evidence for stepwise postglacial sea level rise and an approach to
4 more precise determination of former sea levels on East China Sea Shelf. *MAR*
5 *GEOL*, 348, 52-62, <https://doi.org/10.1016/j.margeo.2013.12.004>, 2014.

6 Xue, C. T.: Extents, type and evolution of Luanhe River fan-delta system, China.
7 *Marine Geology & Quaternary Geology*, 36 (06), 13-22, 2016 (in Chinese with
8 English abstract).

9 Zhou, X.: Basic characteristics and resource classification of subsurface brines in deep-
10 seated aquifers. *Hydrogeology & Engineering Geology*, 40 (5), 4-10, 2013 (in
11 Chinese with English abstract).

12